

Cyclotron resonance and Faraday rotation in graphite

L.A. Falkovsky^{1,2}

¹*L.D. Landau Institute for Theoretical Physics, Moscow 119334, Russia*

²*Institute of the High Pressure Physics, Troitsk 142190, Russia*

(Dated: March 15, 2019)

The optical conductivity of graphite in quantizing magnetic fields is analytically evaluated for frequencies in the range of 10–300 meV, where the electron relaxation processes can be neglected and the low-energy excitations at the "Dirac lines" are more essential. The conductivity peaks are explained in terms of the electron transitions in graphite. Conductivity calculated per one graphite layer tends on average to the universal conductivity of graphene while the frequency is larger than the Landau spacing. The (semi)metal-insulator transformation is possible under doping in high magnetic fields.

PACS numbers: 76.40.+b, 78.20.-e, 81.05.uf

Graphite is usually considered as a layered semimetal composed of the graphene monolayers. Within this assumption, the graphite electron spectrum was evaluated many years ago within the Slonczewski–Weiss–McClure (SWM) theory¹. The so called "Dirac cone" turns into four bands with the twofold degenerate zero mode where electrons and holes are located². The zero-mode dispersion is very small, of the order of 20 meV, in the main-axis direction because the interlayer interaction is weak. Unusual properties of graphite have attracted much attention for more than 50 years. The most accurate method to study the band structure of graphite is a study of the Landau levels (LLs) through experiments such as magneto-optics^{3–9} and magnetotransport^{10–14}. However, the interpretation of the experimental results involves a significant degree of uncertainty since, as noticed by Doezeema *et al*⁴ and Chuang *et al*¹⁵ "it is not clear where the resonances are to be marked."

The SWM theory requires the use of many tight-binding parameters and provides the simple description of observed phenomena either in the semiclassical limit of weak magnetic fields or for high frequencies when the largest tight-binding parameter $\gamma_1 = 0.4$ eV plays the leading role¹⁶. For the relatively strong magnetic fields $B \sim 1\text{--}30$ T and frequencies $\omega \sim 10\text{--}350$ meV, the smaller tight-binding parameters γ_2, γ_5 , and Δ of the order of 20 meV are essential. In this case, any physical property for graphite in magnetic field is represented by an integral over the momentum projection k_z . The SWM model can be simplified assuming that only the integration limits produce the main contributions^{7,15,17}. Such approximation is similar to the theory of magneto-optical effects in topological insulators¹⁸ and graphene¹⁹. However, in the 3d systems, the other features such as the band extrema or the integration limits at the Fermi level can contribute as well. Therefore, the analytical expression for the dynamic conductivity in the presence of magnetic fields is needed for an interpretation of magneto-optics experiments.

In this Letter, we evaluate a formula for the optical conductivity of graphite in the presence of quantizing magnetic fields and results are compared with experi-

ments. We remind the notation for the LLs in graphite using the Hamiltonian in the form of Refs.^{20,21}. The expression for both the longitudinal and Hall dynamical conductivities is given. The (semi)metal-insulator transition is discussed in conclusions.

Neglecting the trigonal wrapping γ_3 , the effective Hamiltonian near the KH -line of the Brillouin zone can be written in the form

$$H(\mathbf{k}) = \begin{pmatrix} \tilde{\gamma}_5 & vk_+ & \tilde{\gamma}_1 & 0 \\ vk_- & \tilde{\gamma}_2 & 0 & 0 \\ \tilde{\gamma}_1 & 0 & \tilde{\gamma}_5 & vk_- \\ 0 & 0 & vk_+ & \tilde{\gamma}_2 \end{pmatrix} \quad (1)$$

where $k_{\pm} = \mp ik_x - k_y$, $v = 1.02 \times 10^8$ cm/s is the intra-layer velocity, and $\tilde{\gamma}_j$ are the functions of k_z :

$$\begin{aligned} \tilde{\gamma}_1 &= 2\gamma_1 \cos(k_z c_0), \quad \tilde{\gamma}_2 = 2\gamma_2 \cos(2k_z c_0), \\ \tilde{\gamma}_5 &= 2\gamma_5 \cos(2k_z c_0) + \Delta \end{aligned}$$

with the distance $c_0 = 3.35$ Å between layers in graphite.

At the magnetic field B , the momentum projections $k_{x,y}$ become the operators with the commutation rule $\{k_+, k_-\} = -2e\hbar B/c$, and we can use the relations

$$k_+ = \sqrt{2|e|\hbar B/c} a, \quad k_- = \sqrt{2|e|\hbar B/c} a^+,$$

involving the creation and annihilation operators. We seek the eigenfunction of the Hamiltonian in the form

$$\psi_{sn}^{\alpha}(x) = \begin{cases} C_{sn}^1 \varphi_{n-1}(x) \\ C_{sn}^2 \varphi_n(x) \\ C_{sn}^3 \varphi_{n-1}(x) \\ C_{sn}^4 \varphi_{n-2}(x) \end{cases} \quad (2)$$

where the Landau number $n \geq 2$ and $\varphi_n(x)$ are orthonormal Hermitian functions with $n \geq 0$. For the eigenvector \mathbf{C}_{sn} , we obtain a system of the linear equations

$$\begin{pmatrix} \tilde{\gamma}_5 - \varepsilon & \omega_c \sqrt{n} & \tilde{\gamma}_1 & 0 \\ \omega_c \sqrt{n} & \tilde{\gamma}_2 - \varepsilon & 0 & 0 \\ \tilde{\gamma}_1 & 0 & \tilde{\gamma}_5 - \varepsilon & \omega_c \sqrt{n-1} \\ 0 & 0 & \omega_c \sqrt{n-1} & \tilde{\gamma}_2 - \varepsilon \end{pmatrix} \times \begin{pmatrix} C_{sn}^1 \\ C_{sn}^2 \\ C_{sn}^3 \\ C_{sn}^4 \end{pmatrix} = 0 \quad (3)$$

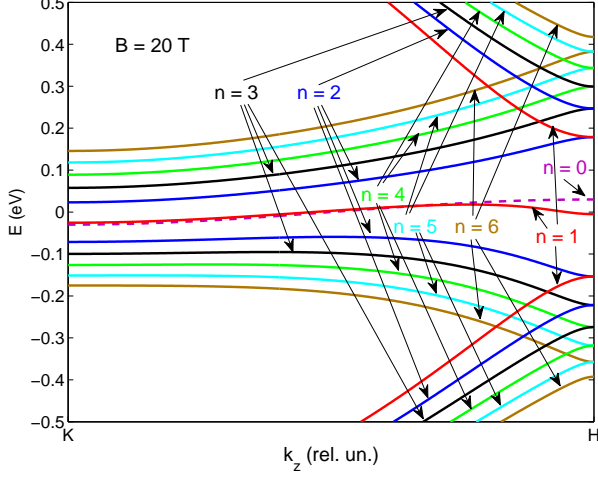


FIG. 1: (Color online) LLs ε_{sn} for $n = 0$ to 6 in four bands s as functions of momentum k_z along the KH -line in the Brillouin zone ($K = 0, H = \pi/2c_0$) at the magnetic field $B = 20$ T using the SWM model with the TB parameters taken from Refs.^{20,21}) and neglecting trigonal warping; the Fermi energy $\varepsilon_F = 0$ eV, and electron transitions are possible between the levels $\varepsilon_{sn} < 0$ and $\varepsilon_{s'n'} > 0$ with the selection rule $\Delta n = \pm 1$.

where $\omega_c = v\sqrt{2|e|\hbar B/c}$.

At each Landau number n , the eigenvalues ε_{sn} of the Hamiltonian are marked by the index of the band $s = 1, 2, 3, 4$ numerating the levels from the bottom. We will use the notation $|sn\rangle$ for levels. LLs with $n \geq 2$ are in every four bands, shown in Fig. 1 as functions of k_z along the KH -line of the Brillouin zone. The eigenvalues are determined by the equation

$$[(\tilde{\gamma}_5 - \varepsilon)(\tilde{\gamma}_2 - \varepsilon) - \omega_c^2(n-1)] \times [(\tilde{\gamma}_5 - \varepsilon)(\tilde{\gamma}_2 - \varepsilon) - \tilde{\gamma}_1^2(\tilde{\gamma}_2 - \varepsilon)^2] = 0.$$

In addition, there are four levels. One of them, $\varepsilon_0 = \tilde{\gamma}_2$, with $n = 0$ and the eigenvector $\mathbf{C}_0 = (0, 1, 0, 0)$. It intersects the Fermi level and belongs to the electron (hole) band near the K (H) point. Other three levels, $s = 1, 2, 3$, are indicated by $n = 1$ with $C_{s1}^4 = 0$. One level, $|11\rangle$, is very close to the level with $n = 0$. This pattern is consistent with Ref.⁶. The level structure at the $K'H'$ -line is similar, therefore each level is fourfold degenerate, twice in spin and twice in the KH and $K'H'$ valleys.

In the region, where $\tilde{\gamma}_1 \gg \tilde{\gamma}_2, \tilde{\gamma}_5$, the two closest bands are written as

$$\varepsilon_{2,3}(n) = \tilde{\gamma}_2 \pm \omega_c^2 \sqrt{n(n-1)}/\tilde{\gamma}_1.$$

The Fermi energy at zero temperature, $T=0$, is determined by equality of electron and hole concentrations given by the sum of integrals

$$n_{h,e} = \frac{\hbar\omega_c^2}{\pi^2 v^2 c_0} \sum_{sn} \int dz \quad (4)$$

over the region in the Brillouin half-zone $z = c_0 k_z$ where electrons and holes are located. As known, the Fermi energy oscillates in the quantum Hall regime. We will consider the relatively strong magnetic fields where the oscillations do not exceed of 2 meV according to the electro-neutrality condition (4).

At finite temperatures the conductivity is expressed in terms of the correlation function²² (for details see Ref.²³)

$$\mathcal{P}(\omega) = T \sum_{\omega_m} \int dx dx' Tr \{ v^i \mathcal{G}(\omega_+, x, x') v^j \mathcal{G}(\omega_-, x', x) \}, \quad (5)$$

where $\mathcal{G}(\omega_+, x, x')$ is the temperature Green's function, $\omega_{\pm} = \omega \pm \omega_m$, and Tr is taken over the $|sn\rangle$ -eigenstates. Using the eigenfunctions (2), we write the Green's function of the Hamiltonian (1)

$$\mathcal{G}^{\alpha\beta}(\omega, x, x') = \sum_{sn} \frac{\psi_{sn}^{\alpha}(x) \psi_{sn}^{*\beta}(x')}{i\omega - \varepsilon_{sn}}.$$

The intralayer-velocity matrix v^i is given by the derivative of the Hamiltonian (1)

$$\mathbf{v} = \frac{\partial H(\mathbf{k})}{\partial \mathbf{k}}. \quad (6)$$

The straightforward calculation of the dynamical conductivity gives

$$\left. \begin{aligned} \sigma_{xx}(\omega) \\ i\sigma_{xy}(\omega) \end{aligned} \right\} = i\sigma_0 \frac{4\omega_c^2}{\pi^2} \sum_{n,s,s'} \int_0^{\pi/2} \frac{dz}{\Delta_{ss'n}} [f(\varepsilon_{s'n+1}) - f(\varepsilon_{s,n})] \times [(\omega + i\Gamma + \Delta_{ss'n})^{-1} \pm (\omega + i\Gamma - \Delta_{ss'n})^{-1}] \times \left\{ |C_{sn}^2 C_{s'n+1}^1|^2 + |C_{sn}^3 C_{s'n+1}^4|^2 \right\}, \quad (7)$$

where $\Delta_{ss'n} = \varepsilon_{sn} - \varepsilon_{s'n+1}$ is the level spacing, $\omega_c = v\sqrt{2|e|\hbar B/c}$ is the cyclotron frequency, and $f(\varepsilon) = [\exp(\frac{\varepsilon - \mu}{T}) + 1]^{-1}$ is the Fermi-Dirac function. The integration over the Brillouin half-zone, $0 < z < \pi/2$, and the summation over the Landau number n as well as the bands s, s' should be done in Eq. (7).

The selection rule $\Delta n = \pm 1$ appears as a result of integration over x and x' in Eq. (5). If the trigonal wrapping is taken into account, the selection rule is changed²⁴. Let us notice that the choice of the selection rule can be done examining the intensities of the cyclotron resonance lines. Our choice corresponds with observations in Refs.^{7,15}.

The results for the longitudinal conductivity $\sigma_{xx}(\omega)$ are shown in Figs. 2, 3, and 4 for the magnetic fields 20 and 30 T. The dynamical Hall conductivity $\sigma_{xy}(\omega)$ shown in Fig. 5 describes the Faraday rotation (see, for instance, Ref.⁹). The formula (7) is valid in the collisionless limit, when the relaxation rate is much less than the frequency, $\Gamma \ll \omega$.

In the calculations, we use the values $\gamma_1 = 390$ meV, $\gamma_2 = -15$ meV, $\gamma_5 = 20$ meV, $\Delta = 35$ meV of Refs.^{20,21}, and set $\Gamma = 5$ meV.

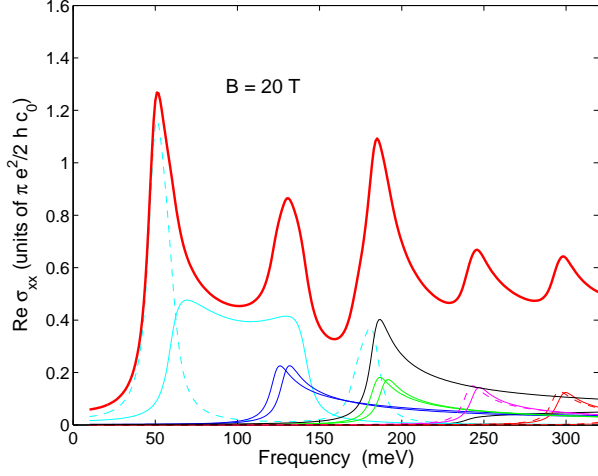


FIG. 2: (Color online) Real part of the longitudinal dynamical conductivity at $B = 20$ T (thick line); the partial contributions of various electron transition are shown in thin lines. Temperature $T = 0.1$ meV is less than the level broadening $\Gamma = 5$ meV.

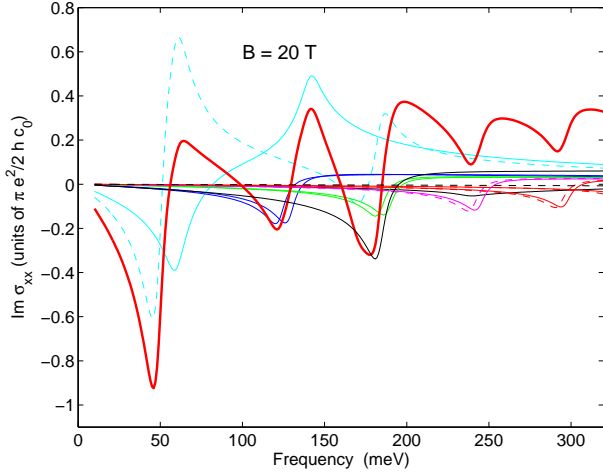


FIG. 3: (Color online) Imaginary part of longitudinal conductivity at $B = 20$ T (thick line) and partial contributions of the electron transitions (thin lines).

The conductivity units of

$$\sigma_0 = \frac{e^2}{4\hbar c_0}$$

have the simple meaning, being the graphene dynamic conductivity $e^2/4\hbar$ multiplied by the number $1/c_0$ of layers within the distance unit in the z -direction. One can see in Fig. 2, that the value of conductivity calculated per one graphite layer tends on average to the graphene universal conductance while the frequency becomes larger than the Landau spacing.

Let us analyze the spectroscopy of the cyclotron reso-

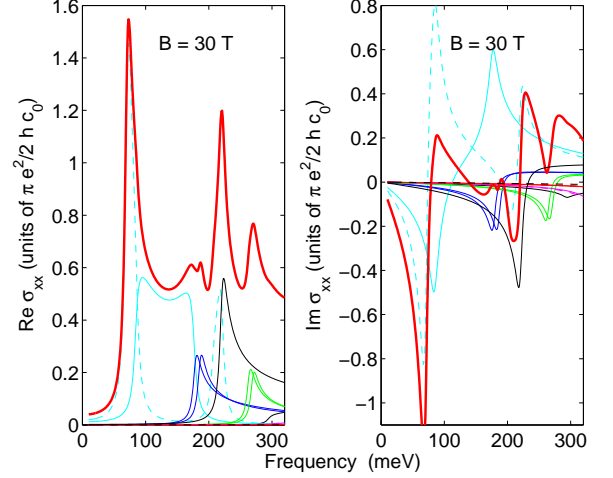


FIG. 4: (Color online) The same as in Figs. 2 and 3 but for $B = 30$ T.

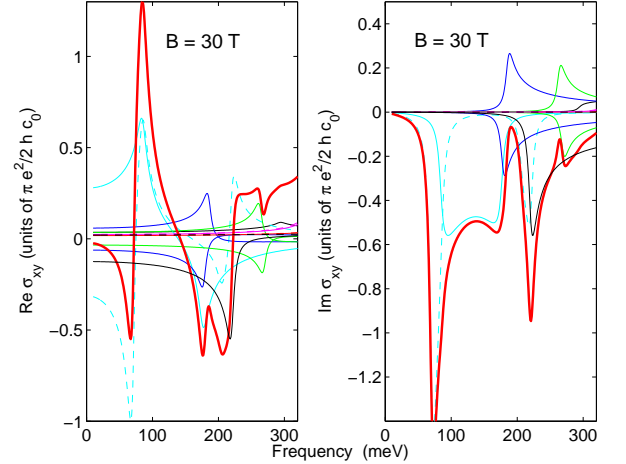


FIG. 5: (Color online) Real and imaginary parts of the dynamical Hall conductivity for $B = 30$ T (thick line) with the partial contributions of various electron transition shown in thin lines.

nances at $B = 20$ T. The line at 298 meV is resulted from the electron transitions $|25\rangle \rightarrow |36\rangle$ and $|26\rangle \rightarrow |35\rangle$ near the K point of the Brillouin zone (see Fig. 1). In the similar way, the 246-meV line includes the $|24\rangle \rightarrow |35\rangle$ and $|25\rangle \rightarrow |34\rangle$ doublet splitted due to the electron-hole asymmetry. However, the more strong line at 187 meV involves other transitions besides the similar $|23\rangle \rightarrow |34\rangle$, $|24\rangle \rightarrow |33\rangle$ doublet. First is the transition $|10\rangle \rightarrow |31\rangle$ near the H point. Second, the transitions $|21\rangle \rightarrow |32\rangle$ from the vicinity of the K point produce the sharp contribution into the 52-meV line, and the transitions between the same levels near the maximum of the $|21\rangle$ -level at $k_z \sim \pi/4c_0$ give the contribution into the 187-meV line. At last the transitions $|22\rangle \rightarrow |21\rangle$ produce the broad

band. The low-frequency and high-frequency sides of the band contribute into the 52-meV and 130-meV lines, correspondingly. The positions of the lines at 20 and 30 T agree very well with observations of Refs.^{7,15}. We do not correct the positions by a variation of the tight-binding parameters. Let us emphasize that the imaginary part of the dynamical conductivity is of the order of the real part.

The optical Hall conductivity $\sigma_{xy}(\omega)$ in the ac regime is shown in Fig. 5. It is evident that the interpretation of the Faraday rotation governed by the conductivity $\sigma_{xy}(\omega)$ is much more complicated in comparison with the longitudinal conductivity.

Notice that the band structure shown in Fig. 1 constrains to consider the (semi)metal-insulator transition while varying the carrier concentration and applying the

magnetic field. The transition induced by the electron-hole interaction has been discussed in Refs.^{10,25,26}. As one can see in Fig. 1, the hole doping can decrease the Fermi energy. While the Fermi level appears between the $|22\rangle$ and $|10\rangle$ levels, the insulator arises with a gap of 34 meV in the magnetic field $B = 20$ T. This transition does not involve the electron-electron interaction and it is resulted due to the layered graphite structure with the small electron dispersion of the zero mode in the k_z -direction.

This work was supported by the Russian Foundation for Basic Research (grant No. 10-02-00193-a) and by the SCOPES grant IZ73Z0.128026 of the Swiss NSF. The author is grateful to the Max Planck Institute for the Physics of Complex Systems for hospitality in Dresden.

-
- ¹ J.W. McClure, Phys. Rev. **108**, 612 (1957); J.C. Slonczewski and P.R. Weiss, Phys. Rev. **109**, 272 (1958).
 - ² G.W. Semenoff, Phys. Rev. Lett. **53**, 2449 (1984).
 - ³ W.W. Toy, M.S. Dresselhaus, G. Dresselhaus, Phys. Rev. B **15**, 4077 (1977).
 - ⁴ R.E. Doezema, W.R. Datars, H. Schaber, A. Van Schyndel, Phys. Rev. B **19**, 4224 (1979).
 - ⁵ Z.Q. Li, S.-W. Tsai, W.J. Padilla, S.V. Dordevic, K.S. Burch, Y.J. Wang, D.N. Basov, Phys. Rev. B **74**, 195404 (2006).
 - ⁶ M. Orlita, C. Faugeras, G. Martinez, D.K. Maude, M.L. Sadowski, M. Potemski, Phys. Rev. Lett. **100**, 136403 (2008).
 - ⁷ M. Orlita, C. Faugeras, J.M. Schneider, G. Martinez, D.K. Maude, M. Potemski, Phys. Rev. Lett. **102**, 166401 (2009).
 - ⁸ M. Orlita, M. Potemski, Semicond. Sci. Technol. **25**, 063001 (2010).
 - ⁹ I. Crassee, J. Levallois, A. L. Walter, M. Ostler, A. Bostwick, E. Rotenberg, T. Seyler, D. van der Marel, A. Kuzmenko, arXiv:1007.5286v1 (2010).
 - ¹⁰ Y. Kopelevich, J.H.S. Torres, R.R. da Silva, F. Mrowka, H. Kempa, P. Esquinazi, Phys. Rev. Lett. **90**, 156402 (2003).
 - ¹¹ I. A. Luk'yanchuk, Y. Kopelevich, Phys. Rev. Lett. **97**, 256801 (2006).
 - ¹² Z. Jiang, Y. Zhang, H.L. Stormer, P. Kim, Phys. Rev. Lett. **99**, 106802 (2007).
 - ¹³ J.M. Schneider, M. Orlita, M. Potemski, D.K. Maude, Phys. Rev. Lett. **102**, 166403 (2009).
 - ¹⁴ A.N. Ramanayaka, R. G. Mani, arXiv:1010.0603v1 (2010).
 - ¹⁵ K.-C. Chuang, A.M.R. Baker, R.J. Nicholas, Phys. Rev. B **80**, 161410(R) (2009).
 - ¹⁶ L.A. Falkovsky, Phys. Rev. B **82**, 073103 (2010).
 - ¹⁷ G. Li, E.Y. Andrei, Nature Phys. **3**, 623 (2007).
 - ¹⁸ W.-K. Tse, A.H. MacDonald, Phys. Rev. B **82**, 161104R (2010).
 - ¹⁹ T. Morimoto, Y. Hatsugai, H. Aoki, Phys. Rev. Lett. **103**, 116803 (2009).
 - ²⁰ B. Partoens and F.M. Peeters, Phys. Rev. B **74**, 075404 (2006).
 - ²¹ A. Grüneis, C. Attaccalite, L. Wirtz, H. Shiozawa, R. Saito, T. Pichler, A. Rubio, Phys. Rev. B **78**, 205425 (2008).
 - ²² A.A. Abrikosov, L.P. Gorkov, I.E. Dzyaloshinski, *Methods of quantum field theory in statistical physics*, Dover Publications, N.Y.
 - ²³ L.A. Falkovsky, A.A. Varlamov, Eur. Phys. J. B **56**, 281 (2007).
 - ²⁴ H. Suematsu, S. Tanuma, J. Phys. Soc. of Jpn. **33**, 1619 (1972).
 - ²⁵ D.V. Khveshchenko, Phys. Rev. Lett. **87**, 246802 (2001).
 - ²⁶ E.V. Gorbar, V.P. Gusynin, V.A. Miransky, L.A. Shovkovy, Phys. Rev. B **66**, 045108 (2002).